Egyptian Journal of Soil Science

http://ejss.journals.ekb.eg/

Simulated Experimental Effect of Bulk Density on Infiltration Rate of China's Loess Plateau

Ahmed E. Talat[1,2], Ruikun Feng[1], Guanheng Liu[1], Jiabo Xie[1], Zekang Cai[1] and **Jian Wang[1*]**

[1] *Institute of Soil and Water Conservation, Northwest A&F University, Yangling 712100, Shaanxi, PR China*
[2] *Soil Science Department, Faculty of Agriculture, Ain Shams University, 11241 Cairo, Egypt*

Understanding the relationship between bulk density (BD) and infiltration rate is crucial for effective water resource management and land use planning in regions with fragile ecosystems such as the Loess Plateau. The study involved selecting five sampling sites, Yangling (YA), Chunhua (CH), Fuxian (FU), Suide (SU), and Shenmu (SH), covering various climate zones and soil types. Laboratory experiments were conducted to simulate different BD values of 1.00, 1.10, 1.20, 1.30, and 1.40 g.cm^{-3} were simulated and three replicates were conducted for each soil at each BD level using soil cylinders and a mini disc infiltrometer (MDI) used to measure infiltration rates under various suction heads over time. Particle size distribution, and soil organic carbon (SOC) content were analyzed for each soil. Results showed infiltration rates decreased with increasing suction head and BD value for all soils. Significant correlations were observed between infiltration parameters and soil constituents (Sand, Silt, and Clay). Also, soil parameters of van Genuchten's model (n, and α) and hydraulic conductivity K, derived from measured data using MDI, varied inversely with BD, high the coefficient of determination (R^2) between the data estimated using MDI and those predicted by the Philip model ranged from (R^2 > 0.832 - 0.969) in most samples, which demonstrated the quality of the data estimated from MDI device, This study demonstrated that increasing BD reduces soil infiltration capacity due to changes in pore structure. The findings provide insights into managing soil and water resources in the ecologically fragile Loess Plateau region by understanding the impacts of compaction on hydrodynamic processes.

Keywords: Soil infiltration rate, Simulate bulk density, Mini disc infiltrometer, Phillip model, Soil parameters, van Genuchten's model, Loess Plateau.

1. Introduction

Soil infiltration rates play an important role in water movement, environmental contaminants, and storage within the vadose zone and affect a variety of hydrodynamic processes, including runoff generation, groundwater recharge, and plant water availability (Rafie and El-Boraie, 2017; Liu et al., 2018; Sun et al., 2018; Chen et al., 2022). Understanding the factors that control infiltration is essential for effective water resource management and land use planning, especially in areas with fragile ecosystems such as the Loess Plateau, China (Chen et al., 2007; Hu and Gao, 2020; Wang et al., 2023). Loess Plateau is characterized by its unique soil type, known as loess, which is highly susceptible to erosion and degradation due to its loose structure and vulnerability to water erosion (Qiang-guo, 2001; Xia et al., 2023). Due to the region's diverse climate, which includes temperate, arid, and semiarid continental monsoon climates, the pattern of precipitation and evaporation varies geographically (Wang et al., 2023; Zhang et al., 2023). There is a considerable amount of precipitation in the summer, with an annual range of 150 mm in the northwest to 800 mm in the southeast. (Yao et al., 2013). These climatic conditions, combined with the topographic features of the region, contribute to the formation of distinct soil landscapes, including flat surfaces, hills, and gullies, across a wide range of elevations (Wei et al., 2022). The infiltration rate is strongly influenced by soil properties, such as bulk density (BD), which is a measure of the compactness of soil (Özdemir et al., 2022; AlSaeedi, 2023). The pore size distribution and porosity of soil are impacted by BD, which has a direct impact on the soil's ability to absorb and transfer water (Lipiec et al., 2006; Mady et al., 2021; Luna-Robles et al., 2024). High BD values can restrict water movement and infiltration, leading to increased surface runoff and decreased water availability for plants (Bettoni et al., 2023; Saffan et al., 2024). Therefore, understanding the relationship between BD and infiltration rate is critical for assessing the

*Corresponding author e-mail: ahmed_ehab2257@nwafu.edu.cn - wangjian@nwafu.edu.cn
Received: 14/10/2024; Accepted: 18/11/2024
DOI: 10.21608/ejss.2024.328370.1886

hydrological function of soils and developing sustainable soil and water conservation strategies in the Loess Plateau (Wang et al., 2023).

Several studies have investigated the effect of BD on soil infiltration in different regions and soil types, for instance (Li et al., 2009; Sun et al., 2018; Liu et al., 2022) observed a negative correlation between BD and infiltration rate. However, these studies didn't focus on laboratory simulation of bulk density and infiltration rate using more than different BD values and suction heads.

This research aims to experimentally investigate the effect of BD on the infiltration rate of soils in the Loess Plateau. The study area includes different climate zones and soil types, representing the region's variability of soil and environmental conditions. Five sampling sites were selected with varying soil characteristics then disturbed soil samples from the soil surface were collected. Laboratory analysis was conducted to determine the particle size distribution and soil organic carbon content of the samples.

The experimental setup involved simulating different bulk density values using soil cylinders and a Mini disc infiltrometer (MDI). The infiltration rate was measured under various suction heads to capture the dynamics of water movement through the soil. The obtained data were analyzed using statistical methods to assess the relationship between BD and infiltration rate. Additionally, the Philip model was employed to predict and evaluate the soil water infiltration process based on the infiltration rate data.

The findings of this research might contribute to a better understanding of the hydrodynamic processes in the Loess Plateau and provide valuable insights into soil and water conservation practices in the region. By elucidating the relationship between BD and infiltration rate, this study will aid in the development of appropriate soil management strategies to mitigate soil erosion, enhance water infiltration, and improve overall ecosystem resilience in the Loess Plateau.

2. Materials and methods

2.1. Description of the study area and experimental soil

The study area within the Loess Plateau in Shaanxi Province, China, is located between (34°17′-38°51′ N, 108°03′-110°25′ E), which has arid, and semiarid continental monsoon climates. Loess Plateau experiences yearly evaporation of 1400 – 2000 mm, annual temperature fluctuations from 3.6 °C in the northwest to 14.3 °C in the southeast, and annual precipitation ranging from 150 mm in the northwest to 800 mm in the southeast, with 55–78% occurring between June and September. The area is encircled by mountains, and at elevations between 100 and 3000 m, the loessial landforms include gullies, hills, and a broad flat area with little erosion. Sampling sites are Yangling (YA), Chunhua (CH), Fuxian (FU), Suide (SU), and Shenmu (SH). The sites represent different climate zones and soil types that were selected on the Loess Plateau in the direction from south to north; Disturbed soil samples were collected from the soil surface, to determine the soil particle size (Sand, Silt, Clay) and soil organic carbon (SOC) content and estimate the infiltration rate at different values of bulk density (BD).

2.2. Laboratory analysis

The disturbed soil samples were air-dried and passed through a 2.0 -mm sieve, before measuring the soil particle composition by laser diffraction (Mastersizer 2000, Malvern Instruments, Malvern, United Kingdom) (Houghton et al., 2002), and through a 0.25 -mm sieve and the dichromate oxidation technique (Nelson and Sommers, 1996) to calculate the SOC content. The soil characterizations are shown in Table 1. We simulated and prepared five soil BD different values (1.00, 1.10, 1.20, 1.30, 1.40 $g.cm^{-3}$), that referred by B1, B2, B3, B4, and B5, respectively. Using three replicates. The dimensions of soil samples were (5 -cm height and 6.5 -cm diameter). The BD was determined using the following formula:

$$BD = \frac{\text{Dry soil mass (g)}}{Volume\ of\ cylinder\ (cm^3)} \quad (1)$$

The volume of the cylinder is:

$$V = \pi r^2 h \quad (2)$$

Where: π = 3.1416; r = radius (half of the diameter) (cm); and h = height of the cylinder (cm).

$$Dry\ soil\ mass(g) = BD \times Volume\ of\ cylinder(cm^3) \quad (3)$$

2.3. Operation of mini disk infiltrometer (MDI)

The mini disc infiltrometer with a disk diameter of 3.1 cm was used in the lab (fig. 1) to run the test for suction heads of -1, -2, -3, -4, and -5 cm, on soil cylinders equipped with soil BD different values. To improve the porous stainless steel disk's contact with the soil sample during infiltration, a tiny quantity of fine sand was added to the upper surface for soil cylinder. As the MDI suction head may be ranged between -0.5 and -7 cm, we can obtain more information about the soil by removing macropores whose air entry value is less than the suction of the device (Abichou and Fatehnia, 2014). The volume in the water reservoir tube was noted at time zero and the change in the water volume was recorded every 30 seconds at regular intervals and measurements were taken continuously until reaching a steady state to calculate the infiltration rate. Cumulative infiltration is obtained by dividing the volume of infiltrating water by the area through which water is infiltrating. We then used Eq.(4) proposed by Zhang (1997) for describing infiltration under disc infiltrometers. Cumulative infiltration and time can be fitted with the function:

$$I = C_1 \sqrt{t} + C_2 t \quad (4)$$

where I is the cumulative infiltration (cm), t is the cumulative time (s), and C_1 and C_2 are constants that are related to the soil sorptivity (S), and the hydraulic conductivity (K) by:

$$C_1 = A_1 K \quad (5)$$

$$C_2 = A_2 S \quad (6)$$

where A1 and A2 are nondimensional coefficients. Consequently, steady infiltration of the soil can be calculated from Eq. (5), The hydraulic conductivity is then computed from:

$$K = \frac{C_1}{A} \quad (7)$$

where C_1 is the slope of the curve of the square root of time versus the cumulative infiltration and A is a value relating the van Genuchten (v.G) parameter for an Genuchten (1980) a given soil type to the suction head and radius of the infiltrometer disc, A is computed from:

$$A = \frac{11.65(n^{0.1}-1)exp[2.92(n-1.9)\alpha h_0]}{(\alpha r_0)^{0.91}} n \geq 1.9 \quad (8)$$

$$A = \frac{11.65(n^{0.1}-1)exp[7.5(n-1.9)\alpha h_0]}{(\alpha r_0)^{0.91}} \quad n < 1.9 \quad (9)$$

where n and α are v.G soil parameters, r_0 is the disk radius, and h_0 is the suction on the disk surface. The v.G soil parameters were obtained from Carsel and Parrish (1988), according to the MDI manufacturer's information.

2.4. The infiltration model evaluation

Philip model was used to predict and evaluate the soil water infiltration process (Dong et al., 2019) using infiltration rate data obtained from MDI. Philip (1957) proposed a model based on a semi-analytical solution of Richards' flow equation (Richards, 1931). In this solution, Philip used a time series to solve the Richards equation. By neglecting the higher-order terms, the Philip model formula is:

$$I = St^{0.5} + At \quad (10)$$

where A is the constant infiltration rate in cm/min, S is the sorptivity in cm/min$^{0.5}$, I is the cumulative infiltration (cm), and t is the infiltration time (s).

Table 1. Main physical and chemical properties of the study sites.

Study sites	SOC	Particle size distribution (%)			Soil texture
		Clay	Silt	Sand	
SH	2.62±0.49	12.93±0.61	13.75±0.65	73.32±0.47	Sandy loam
SU	3.24±0.15	21.91±0.82	29.23±0.89	48.86±1.65	Loam
FU	4.24±0.67	29.16±0.22	35.13±1.17	35.71±1.10	Clay loam
CH	10.87±0.10	32.04±0.89	39.96±1.65	28.00±1.43	Clay loam
YA	29.40±0.27	37.52±0.51	40.94±0.35	21.54±0.97	Clay loam

* SOC soil organic carbon (g kg^{-1}), values represent the mean ± standard error.

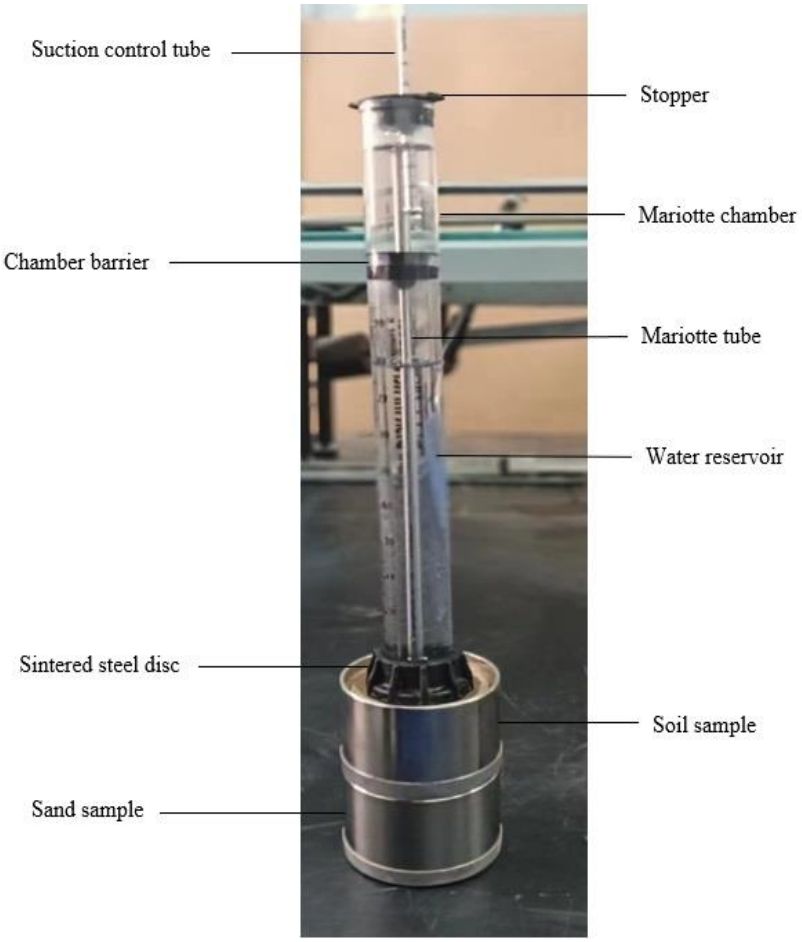

Fig. 1. Mini disc Infiltrometer used for measuring infiltration rate under different BD values.

2.5. Statistical analyses

The infiltration rate parameters under different BD values were analyzed using a one-way analysis of variance (ANOVA). with Duncan's multiple range tests ($p < 0.05$) using SPSS 26 software (IBM SPSS Statistics, Armonk, NY, USA). To find noteworthy variations across groups, post-hoc comparisons were carried out. Groups with the same letter in a column indicate no significant difference ($p < 0.05$). A significant threshold of $p < 0.05$ was established.

3. Results

3.1. The infiltration rate changes with suction head under different BD values

The infiltration velocity is the rate at which water percolates from the soil surface per unit area, or its rate of entry. Figure 2 shows the infiltration velocity of soil with different BD values under suction heads with time using MDI. The variation of soil infiltration rate with time, especially at a suction head of -1 cm at the beginning of the curve was high. It then begins to decrease gradually until it stabilizes, followed by the other suction heads -2, -3, -4, and -5 cm, respectively at sampling sites SH, SU, FU, CH, and YA. In addition to the gradual increase in soil BD values from B1, B2, B3, B4, and B5, respectively, infiltration rates decreased over time in soils with different BD values, mainly due to a decrease in the absolute value of the matric potential and a sharp decrease in soil negative pressure respectively. The soil matric potential gradient starts to gradually diminish after 1 min of infiltration In the initial stages of infiltration, the water entering the soil may be higher, leading to a steeper matric potential gradient. As time progresses, the infiltration rate may decrease due to factors like soil compaction, reduced hydraulic conductivity, or the filling of larger pores, leading to a diminishing gradient. Although the rate of soil infiltration is usually stable, different soil locations with varying textures take varying

amounts of time to achieve steady infiltration. After 7 min, SH soil achieved a steady infiltration state; SU and FU soils did the same after 8 min; and CH and YA soils did so after 9 min.

For the majority of soils, the higher the BD value, the lower the infiltration rate during the infiltration process. The late infiltration curve portion approaches a horizontal straight line, suggesting that BD's impact on the infiltration rate gradually diminishes over time.

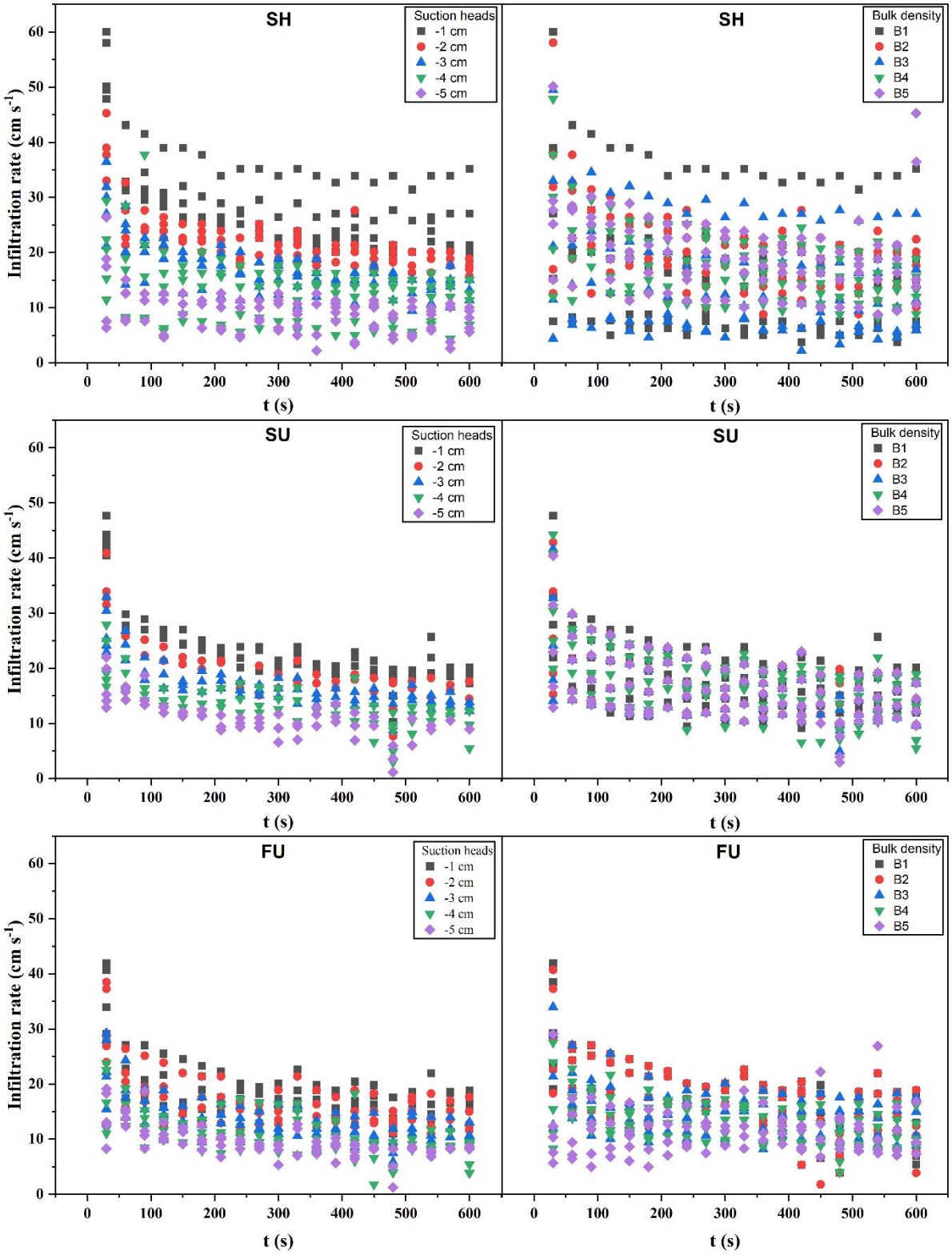

Fig. 2. The infiltration rate of different soils with bulk density values and suction heads with time using MDI.

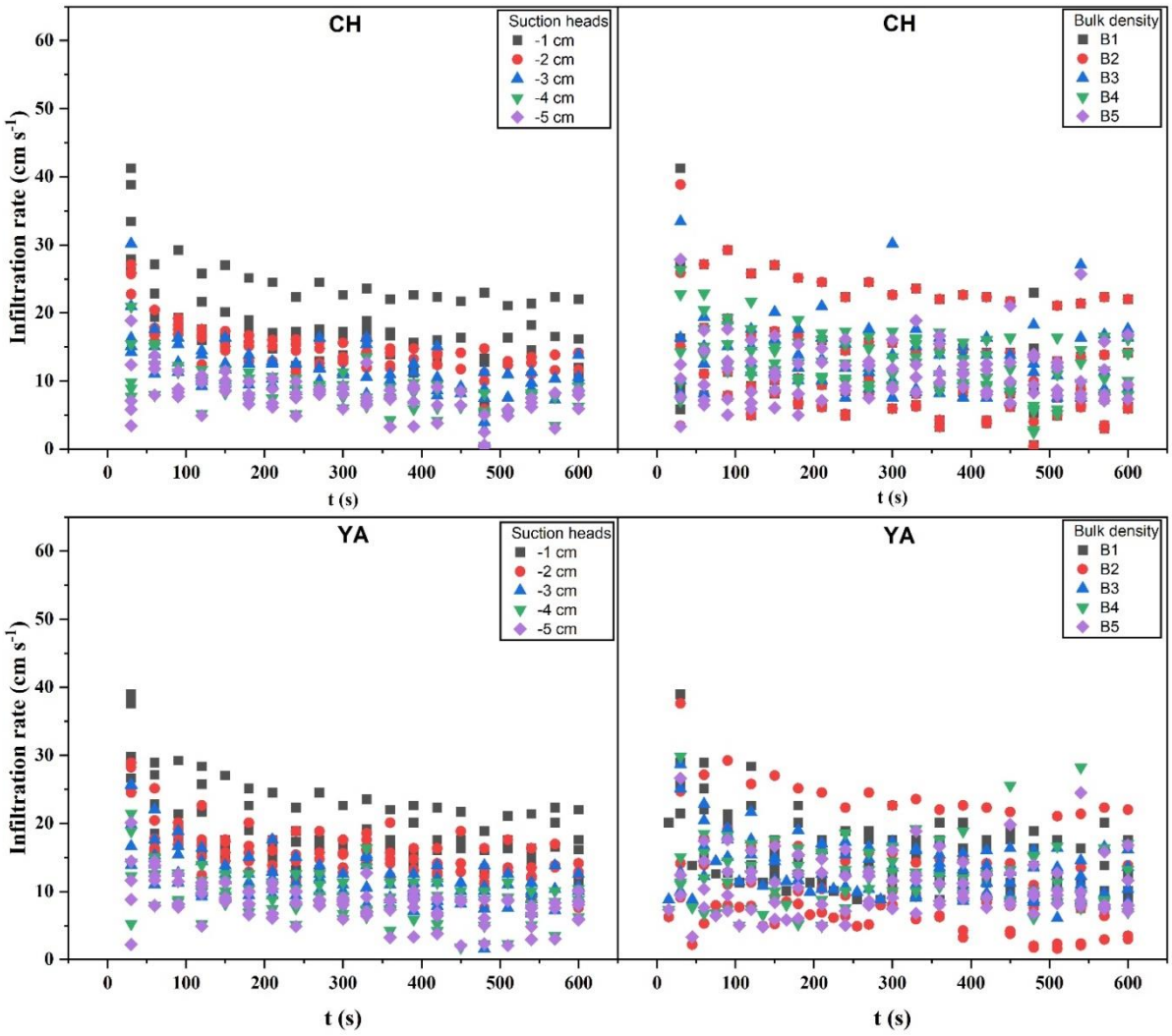

Fig. 2. The infiltration rate of different soils with bulk density values and suction heads with time using MDI (Continued).

3.2. Effect of soil BD on cumulative infiltration

The cumulative infiltration is defined as the total amount of water infiltrated into the soil through the surface per unit area. Figure 3 shows in SH soil when the BD values increased from 1.00 g.cm^{-3} to 1.40 g.cm^{-3}, the cumulative infiltration decreased from 3.25 cm to 2.61 cm, and the Coefficient of determination (R^2 > 0.92), Moreover, we also see that in SU soil when the BD values increased from 1.00 g.cm^{-3} to 1.40 g.cm^{-3}, the cumulative infiltration decreased from 3.01 cm to 2.47 cm, and (R^2 >0.96). In addition, at FU, CH, and YA soils when the BD values increased from 1.00 g.cm^{-3} to 1.40 g.cm^{-3}, the cumulative infiltration decreased from 2.76 cm to 1.99 cm, 2.57 cm to 1.86 cm, and 2.17 cm to 1.74 cm, and (R^2 > 0.99, 0.98 and 0.91), respectively with soils. the soils showed an obvious turning in cumulative infiltration under different BD values. This may be due to the differences in soil texture of the five soils.

3.3. The relationship between infiltration rate parameters and soil properties

Figure 4 displays the Pearson correlation between infiltration rate parameters and soil properties. It shows that BD had a negative correlation with SOC (P = -0.86), and a negative correlation with S, IN, ST, and C1, ranging between (P = -0.74 ≈ -0.90), Sand had a positive correlation with S, IN, ST, and C1, ranging between (P = 0.99 ≈

0.87), and a negative correlation with Silt, Clay, and SOC, ranging between (P = -0.70 ≈ -0.99), Silt had a positive correlation with Clay, and SOC, ranging between (P= 0.99 ≈ 0.63), and a negative correlation with IN, ST, C1, and S, ranging between (P= -0.88 ≈ -0.99), Clay had a positive correlation with SOC (P = 0.78), and a negative correlation with IN, ST, C1, and S, ranging between (P = -0.84 ≈ -0.96), SOC had a negative correlation with IN, ST, C1, and S, ranging between (P = -0.46 ≈ -0.60). Also, IN had a positive correlation with ST, C1, and S, ranging between (P = 0.98 ≈ -0.93), ST had a positive correlation with C1, and S, ranging between (P = 0.98 ≈ 0.94), C1 had a positive correlation with S (P = 0.89).

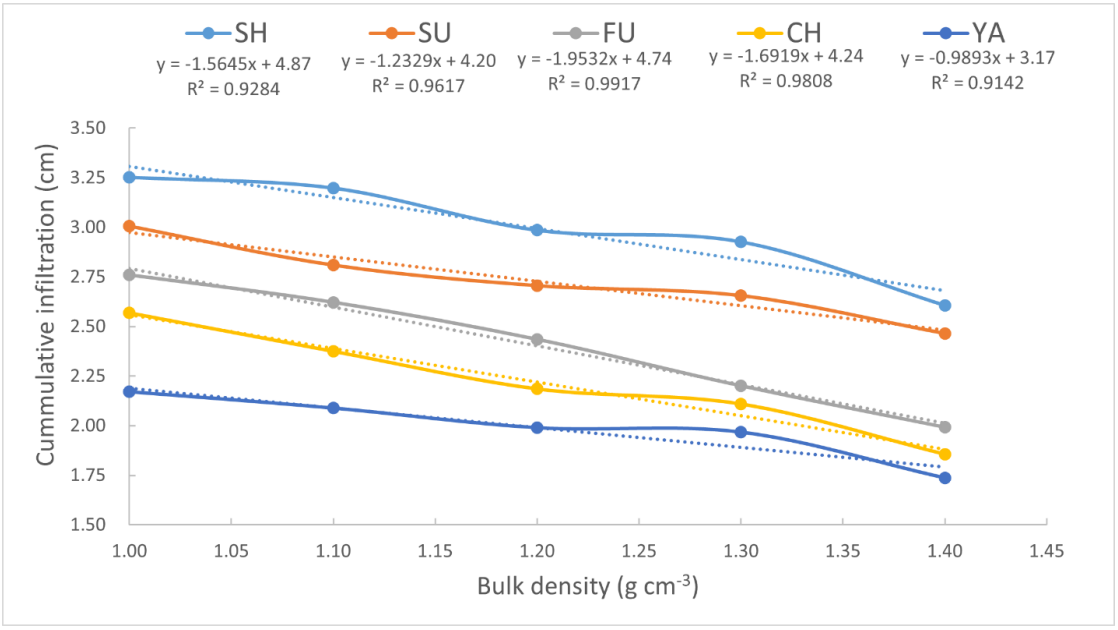

Fig. 3. The relationship between bulk density and cumulative infiltration of different soils.

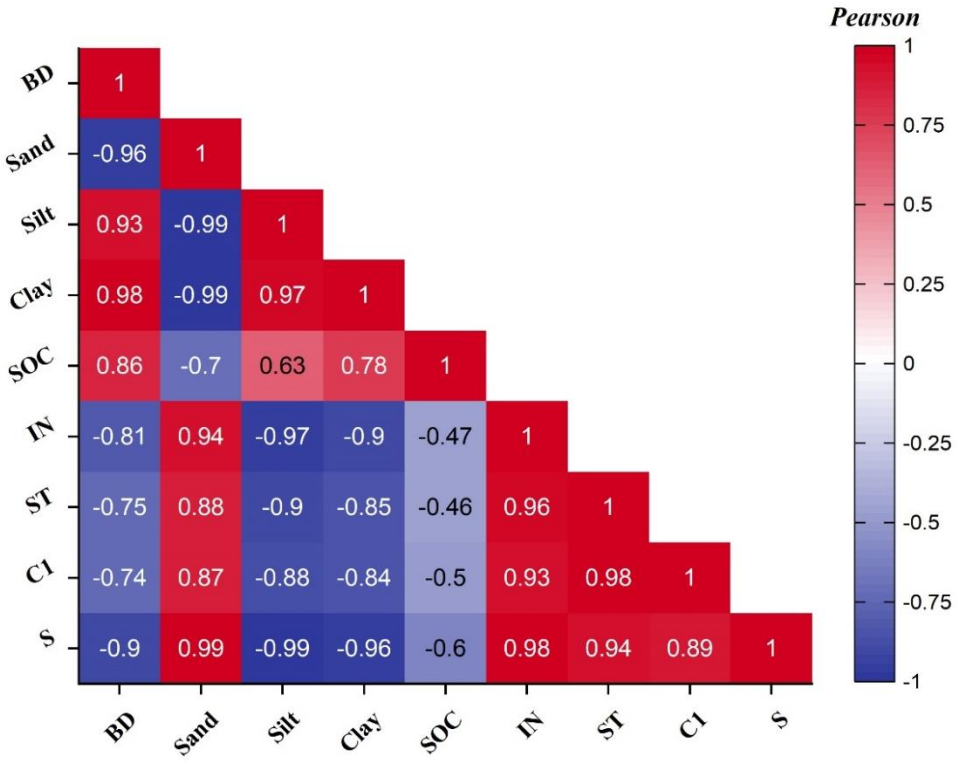

Fig. 4. Triangle heatmap correlation matrix between infiltration rate parameters and soil properties, (BD) soil bulk density, (IN) initial infiltration rate (ST) final infiltration rate, (C1) parameter are related to the soil sorptivity, (S) the soil sorptivity.

3.4. Soil infiltration parameters for different soils and BD values

Table 2 displays Soil infiltration parameters for different soils and BD values, and the coefficient of determination between values measured and predicted for infiltration rate. We find that the highest values of soil parameters n and α at B5 (2.247 and 0.198) in SH, the lowest value at B1 (1.070 and 0.029) in YA, and higher values of 'n' suggest higher water infiltration rates and lower values indicate slower infiltration and higher 'α' values indicate greater water retention capacity and values lower suggest lower water-holding capacity.Also, the highest K value at B1 (9.740) in YA, and the lowest value at B5 (2.160) in SH, higher values of 'K' indicate faster water infiltration and greater soil permeability, and vice versa. This indicates an increase in BD is associated with an increase in the soil parameters n and α. At the same time, a decrease in the K is observed. The coefficient of determination (R^2) values indicates the degree of correlation between the measured values and the predicted values from Philip model. The (R^2) values for the infiltration rate are relatively high values across the different study sites and bulk density values. The R^2 values range from 0.832 to 0.969, suggesting a strong correlation between the measured values obtained from the device and the predicted values using Philip model. The A value is defined as the ratio of the rate of water infiltration into the soil to the rate of water flow out of the soil. Table 3 shows a comparison of the effectiveness of different BD values (B1, B2, B3, B4, and B5) in measuring the A value of a mini-disc infiltration meter at various applied suction heads (-1 to -5 cm). The table shows the average A values for each BD value at each applied suction head, along with their standard deviations. We found that the A values are generally higher for soils with higher BD values (i.e., B5, B4, and B3 have higher A values than B2 and B1), this suggests that these soils may be more effective at measuring the infiltration rate of water through the soil profile, this relationship could be due to the compactness of the soil, which affects how easily water can penetrate through it. Soils with higher BD are typically more compacted, which can slow down water infiltration but might provide more accurate measurements due to the decreased permeability. However, it's also worth noting that the A values can vary significantly between soils even when they have similar BD values. For example, B1 has an A value of 5.75±0.60 a, while B2 has an A value of 7.35±1.65 a. This suggests that there may be some variability in the performance of different soils, even if they have similar BD values.

3.5. Effect of BD values and SOC content on saturated hydraulic conductivity

Soil hydraulic conductivity is a crucial parameter that characterizes the ability of soil to transmit water. It is influenced by various soil properties, such as texture, structure, porosity, and organic matter content.

Figure 5 shows the relationship between observed and model-fitted values of saturated hydraulic conductivity (Ks) with BD values and SOC content for different soil studies. Ks varied considerably between replicates for most soil studies (Fig. 5 a, b, c, d). By comparing the observed values with the model-fitted values, the accuracy and reliability of the model can be evaluated. Higher bulk density often leads to reduced pore space and decreased hydraulic conductivity. In addition, the study demonstrated that increasing SOC content enhanced hydraulic conductivity by promoting soil aggregate stability and pore formation. SOC content, on the other hand, affects soil structure, water-holding capacity, and nutrient availability, it is generally associated with improved soil aggregation and increased hydraulic conductivity. The relationship between these variables is complex and site-specific, requiring the use of models to better understand and predict hydraulic conductivity under different conditions.

Table 2. Soil infiltration parameters for different soils and BD values, and the coefficient of determination between values measured and predicted for infiltration rate.

Study sites	BD	n	α	K	R^2
SH	B1	1.972	0.164	9.740	0.942
	B2	2.026	0.168	8.448	0.881
	B3	2.044	0.169	6.220	0.883
	B4	2.067	0.179	5.014	0.933
	B5	2.247	0.198	4.491	0.969
SU	B1	1.635	0.150	5.423	0.905
	B2	1.799	0.154	4.744	0.931
	B3	1.862	0.158	3.940	0.891
	B4	1.947	0.160	3.460	0.888
	B5	1.964	0.162	3.328	0.923
FU	B1	1.129	0.035	4.837	0.874
	B2	1.189	0.044	4.109	0.952
	B3	1.327	0.074	4.084	0.881
	B4	1.527	0.135	3.469	0.922
	B5	1.568	0.148	2.558	0.965
CH	B1	1.076	0.035	4.635	0.873
	B2	1.186	0.039	3.273	0.967
	B3	1.196	0.055	3.956	0.959
	B4	1.474	0.078	2.759	0.965
	B5	1.553	0.142	2.261	0.862
YA	B1	1.070	0.029	4.247	0.832
	B2	1.136	0.039	3.122	0.944
	B3	1.192	0.047	3.347	0.938
	B4	1.451	0.074	2.292	0.940
	B5	1.538	0.141	2.160	0.964

* n and α are van Genuchten parameters and reflect the index of the empirical infiltration (cm^{-1}), n influences the distribution of pore sizes in the soil and affects the shape of the curve, while α determines the pressure at which air enters the soil pores, K is equal to the infiltration rate at the end of the first period ($cm\ h^{-1}$).

Table 3. Mini-disc infiltrometer data for A value at applied suction heads between −1 to −5 cm for soil BD values.

	A					
BD	**1-**	**-2**	**-3**	**-4**	**-5**	**CV**
B1	5.75±0.60 a	3.42±0.33 a	2.50±0.24 a	1.87±0.31 a	1.14±0.27 a	0.700±0.025 a
B2	7.35±1.65 a	3.79±0.33 a	2.58±0.27 a	1.98±0.31 a	1.27±0.27 a	0.693±0.067 a
B3	8.44±1.67 a	3.97±0.27 a	2.77±0.30 a	2.04±0.29 a	1.46±0.28 a	0.688±0.065 a
B4	9.46±1.73 a	4.28±0.24 ab	2.88±0.30 a	2.14±0.31 a	1.58±0.31 a	0.700±0.058 a
B5	10.57±2.15a	5.32±0.70 b	2.97±0.28 a	2.21±0.29 a	1.71±0.33 a	0.697±0.054 a

* The same letters following the numbers indicate there was no significant difference between the two datasets based on Duncan's multiple-range test results ($p < 0.05$).

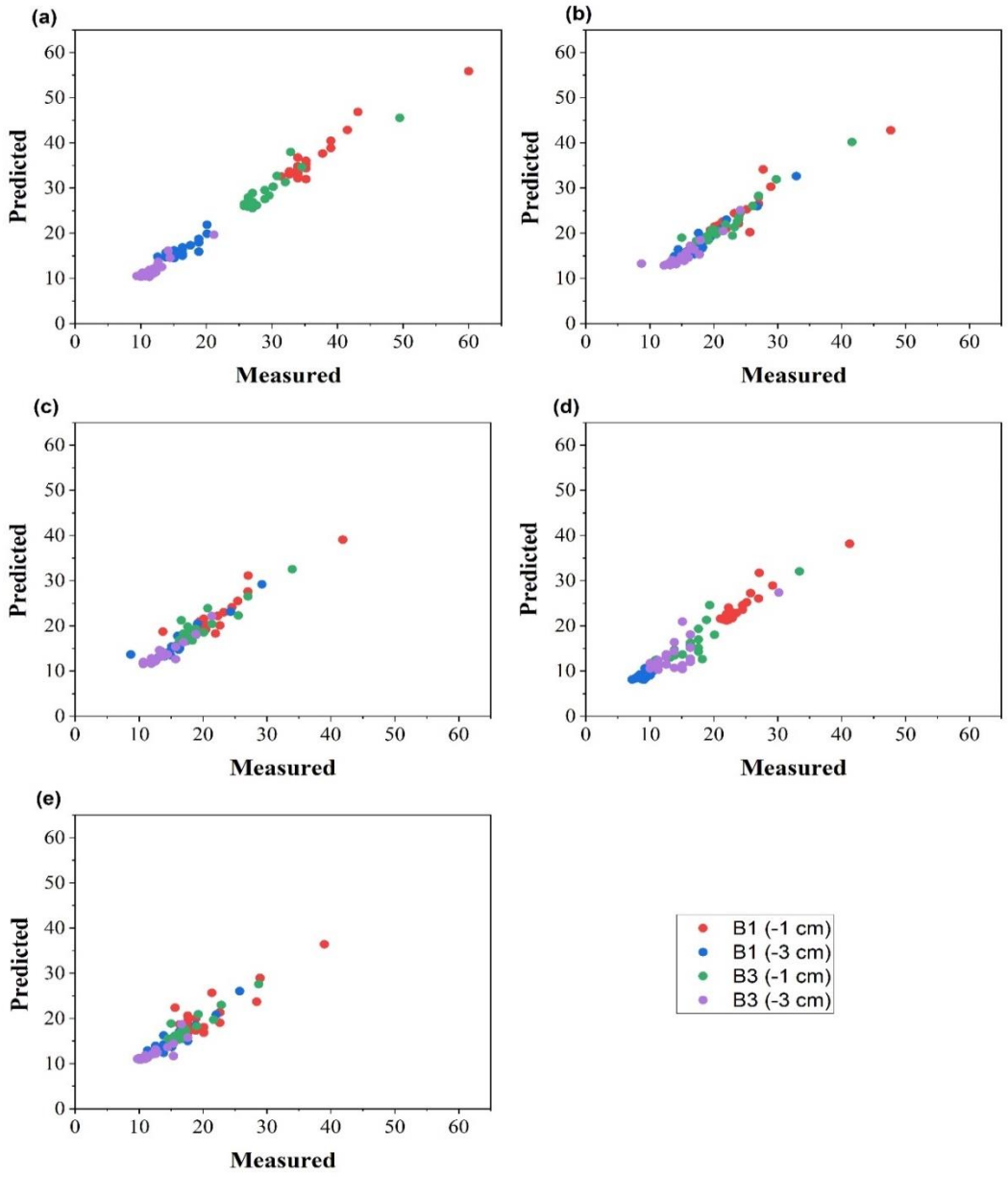

Fig. 5. Comparison of predicted infiltration rate by the Phillip model with the measured results by MDI for bulk density (B1 and B3) under suction heads (-1 cm and -3 cm) different soils in (a) SH, (b) SU, (c) FU, (d) CH, and (e) YA.

4. Discussion

The infiltration rate is a reflection of the soil's infiltration performance and the BD structure, which has a significant impact on the soil's ability to store and drain water. Water retention in the soil is challenging, though, if the infiltration capacity s excessively high, it represents the ability of the soil to absorb water and is influenced by factors such as soil characteristics, land use, slope, vegetation cover, and antecedent soil moisture conditions. The effect of BD on water infiltration capacity is determined by the number of macropores present. According to Darcy's seepage law of unsaturated soil states that soil hydraulic conductivity and soil water potential gradient determine the infiltration of soil moisture, whereas soil texture, BD, structure, moisture content, and matric potential primarily determine soil hydraulic conductivity (Wang et al., 2016; Talat et al., 2020; Omran et al., 2023). Soil matric potential is the primary factor influencing the initial stage of infiltration. A larger initial infiltration rate is the result of a high matric potential gradient at the interface of the soil column, as well as a large soil negative pressure caused by the low initial soil water content. BD affects the size and distribution of soil pores, which in turn impacts the infiltration rate of soil. The gravitational potential gradually influences the

infiltration process after water saturation of upper soil layer, then the infiltration rates decrease rapidly due to soil properties such as the texture of the soil and bulk density (Dong et al., 2019).

Figure 5 presents the predicted infiltration rate by the Phillip model and the measured values using MDI for different soils under BD vales. Generally both the predicted and measured ones are consistent. However, there are some variations in the predicted infiltration rate by the Phillip model for different soils, which may be due to differences in the soil properties (Mishra et al., 2003; Dahak et al., 2022). The infiltration rate was found to change with suction heads under different BD values. The infiltration rate decreased over time, primarily due to a rapid decrease in the the matric potential. Additionally, an increase in soil BD values led to a decrease in the infiltration rate, so our experimental result in agreement with previous research that has shown a negative correlation between BD and infiltration capacity (Yang et al., 2011). Cumulative infiltration was also influenced by soil BD values. Higher BD values resulted in lower cumulative infiltration values. This observation is supported by studies of (Atta-Darkwa et al., 2022; Abdel-Sattar et al., 2023). Their results demonstrated a negative relationship between BD and cumulative infiltration. Furthermore, the study investigated the relationship between infiltration rate parameters and soil properties. The results showed that BD had a positive correlation with Clay, and Silt, while it had a negative correlation with Sand, SOC, IN, ST, and S. This finding aligns with previous research that has reported similar correlations between soil properties and infiltration parameters (Leung et al., 2018; Dias et al., 2023).

We found that there is an inverse relationship between the soil infiltration parameters A and K, that as BD increases, K decreases with different soil textures, indicating slower infiltration rates. Similarly, A values are generally higher for soils with higher BD (B5, B4, and B3) compared to those with higher BD (B2-B1). Shi et al. (2022) found a significant negative correlation between A and K in soils, this is consistent with our results. Conversely, Ren et al. (2016) found positive correlations between A and K in some soil textures, this is attributed to macropore flow dominating the infiltration process. The presented data also included soil infiltration parameters for different soils and BD values. The parameters n and α were found to increase with higher BD values, indicating lower water infiltration rates and less water retention capacity. Conversely, the parameter K which represents soil permeability, decreased with higher BD values, suggesting slower infiltration and lower permeability. These results are consistent with the findings of studies conducted by Kool et al. (2019) and Castellini et al. (2020), which reported similar trends in infiltration parameters with varying BD.

5. Conclusion

In this study, the influence of soil BD values on infiltration rate under different suction heads and soil textures was investigated. The measurement was conducted using MDI device, and predicting its data and evaluating it using the Philip model, which provided valuable insights into the soil infiltration rate. The results demonstrate that the infiltration rate of different soils varies with different suction heads. Initially, the infiltration rate decreased gradually until it stabilized at various suction heads depending on the BD and soil textures. The final infiltration rates differed among different soil types. There was a clear negative relationship between BD and the infiltration rate. Generally, as the BD value increased, the infiltration rate decreased. This trend was observed across different soil types. Various soil properties, such as sand, silt, clay, and SOC, showed correlations with infiltration rate parameters. The study also analyzed soil infiltration parameters, including the van Genuchten parameters n and α, as well as the K value. These parameters reflect water infiltration rates, water retention capacity, and soil permeability. These observations highlight the effect of soil BD values on infiltration rate using different soil textures. It is important to note that the results obtained in this study are specific to some soils in the loess plateau. Other different regions and soil types may exhibit variations in soil hydrodynamic properties, leading to different, effects of soil BD on soil infiltration rate. Future research should consider these variations and employ more accurate experimental methods to better understand hydrodynamic changes in soil systems. Overall, this study provides valuable insights into the influence of soil BD on soil infiltration rate and contributes to water and soil resource management in arid and semi-arid regions.

List of abbreviations:

BD (g cm^{-3}): Bulk density in grams per cubic centimeter
SOC (g kg^{-1}): Soil organic carbon in grams per kilogram
K (cm h^{-1}): infiltration rate in centimeters per hour
IN (cm h^{-1}): initial infiltration in centimeters per hour

I (cm): cumulative infiltration in centimeter
S (cm $min^{-0.5}$): soil sorptivity in centimeters per half minute
n and α (cm^{-1}): are van Genuchten parameters and reflect the index of the empirical infiltration per centimeters

Declarations

Ethics approval and consent to participate

Consent for publication: The article contains no such material that may be unlawful, defamatory, or which would, if published, in any way whatsoever, violate the terms and conditions as laid down in the agreement.

Availability of data and material: Not applicable.

Competing interests: The authors declare that they have no conflict of interest.

Funding: This work was supported by the National Natural Science Foundation of China (42377332), and the Funding of Rejuvenate the Inner Mongolia with Science and Technology (2022EEDSKXM005-01), and the National Key Research and Development Program of China (2022YFF1300801).

Authors' contributions: AET responsible for research idea, methodology, and writing the manuscript. RF, GL and JX support in experiment design and overall coordination, ZC and JW general revisions and corrections. All authors read and agree for submission of manuscript to the journal.

References

Abdel-Sattar, M., Al-Obeed, R. S., Al-Hamed, S. A., and Aboukarima, A. M. (2023). Experimental and Modeling Evaluation of Impacts of Different Tillage Practices on Fitting Parameters of Kostiakov's Cumulative Infiltration Empirical Equation. *Water*, 15(14), 2673. doi:10.3390/w15142673.

Abichou, T., and Fatehnia, M. (2014). Comparison of the methods of hydraulic conductivity estimation from mini disk infiltrometer. *Electron J Geotech Eng*, 19, 1047-1061. https://www.academia.edu/download/33699045/Milad_Fatehnia-EJGE.pdf.

AlSaeedi, A. H. (2023). Assessment and development of pedotransfer functions to estimate soil saturated hydraulic conductivity in arid soils with application to GIS mapping in the Al-Ahsa Oasis, Saudi Arabia. *Egyptian Journal of Soil Science*, 63(4), 581-591. doi: 10.21608/EJSS.2023.227275.1631

Atta-Darkwa, T., Asare, A., Amponsah, W., Oppong, E. D., Agbeshie, A. A., Budu, M., ... and Quaye, D. N. D. (2022). Performance evaluation of infiltration models under different tillage operations in a tropical climate. *Scientific African*, 17, e01318. doi:10.1016/j.sciaf.2022.e01318.

Bettoni, M., Maerker, M., Bosino, A., Conedera, M., Simoncelli, L., and Vogel, S. (2023). Land use effects on surface runoff and soil erosion in a southern Alpine valley. *Geoderma*, 435, 116505. doi: 10.1016/j.geoderma.2023.116505.

Carsel, R. F., and Parrish, R. S. (1988). Developing joint probability distributions of soil water retention characteristics. *Water resources research*, 24(5), 755-769. doi:10.1029/WR024i005p00755.

Castellini, M., Vonella, A. V., Ventrella, D., Rinaldi, M., and Baiamonte, G. (2020). Determining soil hydraulic properties using infiltrometer techniques: An assessment of temporal variability in a long-term experiment under minimum-and no-tillage soil management. *Sustainability*, 12(12), 5019. doi:10.3390/su12125019.

Chen, L., Wang, H., Liu, C., Cao, B., and Wang, J. (2022). Use of multifractal parameters to determine soil particle size distribution and erodibility of a physical soil crust in the Loess Plateau, China. *Catena*, 219, 106641. doi: 10.1016/j.catena.2022.106641.

Chen, L., Wei, W., Fu, B., and Lü, Y. (2007). Soil and water conservation on the Loess Plateau in China: review and perspective. *Progress in Physical Geography*, 31(4), 389-403. doi: 10.1177/0309133307081290.

Dahak, A., Boutaghane, H., and Merabtene, T. (2022). Parameter estimation and assessment of infiltration models for Madjez Ressoul Catchment, Algeria. *Water*, 14(8), 1185. doi:10.3390/w14081185.

Dias, P. M. S., Portela, J. C., Gondim, J. E. F., Batista, R. O., Rossi, L. S., Medeiros, J. L. F., ... and do Nascimento, C. M. (2023). Soil Attributes and Their Interrelationships with Resistance to Root Penetration and Water Infiltration in Areas with Different Land Uses in the Apodi Plateau, Semiarid Region of Brazil. *Agriculture*, 13(10), 1921. doi:10.3390/agriculture13101921.

Dong, Q. G., Han, J. C., Zhang, Y., Li, N., Lei, N., Sun, Z. H., ... and He, J. (2019). Water infiltration of covering soils with

different textures and bulk densities in gravel-mulched areas. *Applied Ecology & Environmental Research,* 17(6). doi:10.15666/aeer/1706_1403914052.

Houghton, J. I., Burgess, J. E., and Stephenson, T. (2002). Off-line particle size analysis of digested sludge. *Water Research,* 36(18), 4643-4647. doi:10.1016/S0043-1354(02)00157-4.

Hu, Y., and Gao, M. (2020). Evaluations of water yield and soil erosion in the Shaanxi-Gansu Loess Plateau under different land use and climate change scenarios. *Environmental Development,* 34, 100488. doi: 10.1016/j.envdev.2019.100488.

Kool, D., Tong, B., Tian, Z., Heitman, J. L., Sauer, T. J., and Horton, R. (2019). Soil water retention and hydraulic conductivity dynamics following tillage. *Soil and tillage research,* 193, 95-100. doi:10.1016/j.still.2019.05.020.

Leung, A. K., Boldrin, D., Liang, T., Wu, Z. Y., Kamchoom, V., and Bengough, A. G. (2018). Plant age effects on soil infiltration rate during early plant establishment. *Géotechnique,* 68(7), 646-652. doi: 10.1680/jgeot.17.T.037.

Li, Z., Wu, P., Feng, H., Zhao, X., Huang, J., and Zhuang, W. (2009). Simulated experiment on effect of soil bulk density on soil infiltration capacity. *Transactions of the Chinese Society of Agricultural Engineering,* 25(6), 40-45. doi: 10.3969/j.issn.1002-6819.2009.06.007.

Lipiec, J., Kuś, J., Słowińska-Jurkiewicz, A., and Nosalewicz, A. (2006). Soil porosity and water infiltration as influenced by tillage methods. *Soil and Tillage research,* 89(2), 210-220. doi: 10.1016/j.still.2005.07.012.

Liu, Y., Guo, Y., Long, L., and Lei, S. (2022). Soil water behavior of sandy soils under semiarid conditions in the Shendong mining area (China). *Water,* 14(14), 2159. doi:10.3390/w14142159.

Liu, Z., Ma, D., Hu, W., and Li, X. (2018). Land use dependent variation of soil water infiltration characteristics and their scale-specific controls. *Soil and Tillage Research,* 178, 139-149. doi: 10.1016/j.still.2018.01.001.

Luna Robles, E. O., Alvarez Favela, D. O., Rodriguez Reta, I., Torres Siqueiros, U., Hernandez, F. J., and Bejar Pulido, S. J. (2024). A case study of the physical and hydrological characteristics of the soil after the occurrence of forest fires in Durango, Mexico. *Egyptian Journal of Soil Science,* 64(4), 1511-1524. doi: 10.21608/EJSS.2024.307105.1822

Mady, A. Y., Shein, E. V., Abrosimov, K. N., and Skvortsova, E. (2021). X-ray computed tomography: Validation of the effect of pore size and its connectivity on saturated hydraulic conductivity. *Soil & Environment,* 40(1). doi:10.25252/SE/2021/182420.

Mishra, S. K., Tyagi, J. V., and Singh, V. P. (2003). Comparison of infiltration models. *Hydrological processes,* 17(13), 2629-2652. doi:10.1002/hyp.1257.

Nelson, D. W., and Sommers, L. E. (1996). Total carbon, organic carbon, and organic matter. Methods of soil analysis: Part 3 *Chemical methods,* 5, 961-1010. doi:10.2136/sssabookser5.3.c34.

Omran, W. M., El-Mageed, A., Taia, A., Sweed, A. A., and Awad, A. A. (2023). A modified equation for fitting the shape feature of the entire soil water characteristic curves. *Egyptian Journal of Soil Science,* 63(1), 15-34. doi: 10.21608/EJSS.2022.164765.1541

Özdemir, N., Demir, Z., and Bülbül, E. (2022). Relationships between some soil properties and bulk density under different land use. *Soil Studies,* 11(2), 43-50. doi:10.21657/soilst.1218353.

Philip, J. R. (1957). The theory of infiltration: 1. The infiltration equation and its solution. *Soil science,* 83(5), 345-358. doi:10.1016/B978-1-4831-9936-8.50010-6.

Qiang-guo, C. A. I. (2001). Soil erosion and management on the Loess Plateau. *Journal of Geographical Sciences,* 11, 53-70. doi: 10.1007/BF02837376.

Rafie, R. M., and El-Boraie, F. M. (2017). Effect of drip irrigation system on moisture and salt distribution Patterns under North Sinai Conditions. *Egyptian Journal of Soil Science,* 57(3), 247-260. doi: 10.21608/ejss.2017.4158

Ren, Z., Zhu, L., Wang, B., and Cheng, S. (2016). Soil hydraulic conductivity as affected by vegetation restoration age on the Loess Plateau, China. *Journal of Arid Land,* 8, 546-555. doi: 10.1007/s40333-016-0010-2.

Richards, L. A. (1931). Capillary conduction of liquids through porous mediums. *physics,* 1(5), 318-333. doi:10.1063/1.1745010.

Saffan, M. M., El-Henawy, A. S., Agezo, N. A., and Elmahdy, S. (2024). Effect of irrigation water quality on chemical and physical properties of soils. *Egyptian Journal of Soil Science,* 64(4). doi: 10.21608/EJSS.2024.295064.1784

Shi, S., Zhao, F., Ren, X., Meng, Z., Dang, X., and Wu, X. (2022). Soil infiltration properties are affected by typical plant

communities in a semi-arid desert grassland in China. *Water*, 14(20), 3301. doi:10.3390/w14203301.

Sun, D., Yang, H., Guan, D., Yang, M., Wu, J., Yuan, F., ... and Zhang, Y. (2018). The effects of land use change on soil infiltration capacity in China: A meta-analysis. *Science of the Total Environment*, 626, 1394-1401. doi: 10.1016/j.scitotenv.2018.01.104.

Talat, A. E., Galal, M. E., Yeser, A., and Saad El-Dein, A. A. (2020). Quantifying the hydraulic properties of some Egyptian soils using RETC code. *Arab Universities Journal of Agricultural Sciences*, 28(2), 685-694. doi: 10.21608/ajs.2020.30020.1208.

van Genuchten, M. T. (1980). A closed-form equation for predicting the hydraulic conductivity of unsaturated soils. *Soil science society of America journal*, 44(5), 892-898. doi.org/10.2136/sssaj1980.03615995004400050002x

Wang, J., Watts, D. B., Meng, Q., Zhang, Q., Wu, F., and Torbert, H. A. (2016). Soil water infiltration impacted by maize (Zea mays L.) growth on sloping agricultural land of the Loess Plateau. *Journal of Soil and Water Conservation*, 71(4), 301-309. doi:10.2489/jswc.71.4.301.

Wang, L., Song, X., Li, L., Zhao, X., Meng, P., Fu, C., ... and Li, H. (2023). Research on green water components and potential evaluation framework based on MIKE SHE model–A case study in the Loess Plateau of China. *Ecological Indicators*, 154, 110613. doi:10.1016/j. ecolind.2023.110613.

Wang, L., Wang, J., He, F., Wang, Q., Zhao, Y., Lu, P., ... and Jia, X. (2023). Spatial–temporal variation of extreme precipitation in the Yellow–Huai–Hai–Yangtze Basin of China. *Scientific Reports*, 13(1), 9312. doi:10.1038/s41598-023-36470-0.

Wei, H., Xiong, L., Zhao, F., Tang, G., and Lane, S. N. (2022). Large-scale spatial variability in loess landforms and their evolution, Luohe River Basin, Chinese Loess Plateau. *Geomorphology*, 415, 108407. doi: 10.1016/j.geomorph.2022.108407.

Xia, J., Ren, D., Wang, X., Xu, B., Zhong, X., and Fan, Y. (2023). Ecosystem Quality Assessment and Ecological Restoration in Fragile Zone of Loess Plateau: A Case Study of Suide County, China. *Land*, 12(6), 1131. doi:10.3390/land12061131.

Yang, J. L., and Zhang, G. L. (2011). Water infiltration in urban soils and its effects on the quantity and quality of runoff. *Journal of soils and sediments*, 11, 751-761. doi:10.1007/s11368-011-0356-1.

Yao, Y., Wang, R., Yang, J., Yue, P., Lu, D., Xiao, G., ... and Liu, L. (2013). Changes in terrestrial surface dry and wet conditions on the Loess Plateau (China) during the last half century. *Journal of Arid Land*, 5, 15-24. doi: 10.1007/s40333-013-0137-3.

Zhang, J., Chen, H., Nie, Y., Fu, Z., Lian, J., Luo, Z., and Wang, F. (2023). Temporal variations of precipitation driven by local meteorological parameters in southwest China: Insights from 9 years of continuous hydro-meteorological and isotope observations. *Journal of Hydrology: Regional Studies*, 46, 101345. doi: 10.1016/j.ejrh.2023.101345.

Zhang, R. (1997). Determination of soil sorptivity and hydraulic conductivity from the disk infiltrometer. *Soil Science Society of America Journal*, 61(4), 1024-1030. doi:10.2136/sssaj1997.03615995006100040005x.